Article

Insights into the Adsorption Performance of Emerging Contaminants on Granular Activated Carbon

Sang-Hoon Lee [1,†], Namgyu Kim [2,†] and Donghee Park [3,*]

1   Water Environmental Engineering Research Division, National Institute of Environmental Research, Incheon 22689, Republic of Korea; lsh17007@hanmail.net
2   Environment Solution Research 2 Team, GS Engineering & Construction Corp., 33 Jong-ro, Jongro-gu, Seoul 03159, Republic of Korea; gyustar86@naver.com
3   Department of Environmental and Energy Engineering, Yonsei University, 1 Yonseidae-gil, Wonju 26493, Republic of Korea
*   Correspondence: dpark@yonsei.ac.kr; Tel.: +82-33-760-2435; Fax: +82-33-760-2571
†   These authors contributed equally to this work.

Abstract: Emerging contaminants are being detected at a high frequency, posing significant environmental and human health challenges. This study aimed to investigate the potential of using commercial granular activated carbon for adsorbing nine aqueous emerging contaminants (carbamazepine, phenacetin, pentoxifylline, norfloxacin, iprobenfos, isoprothiolane, metolachlor, tebuconazole, and hexaconazole). The adsorption study involved employing kinetic and isotherm models, using various concentrations of emerging contaminants and sorbents in a batch system. Additionally, the study explored the correlation between the characteristics of emerging contaminants and their adsorption values, which displayed a relatively linear relationship. While some previous papers have evaluated the performance of one or two substances, there is a lack of research on the adsorption mechanisms of all nine aqueous emerging contaminants. Therefore, the findings from this study on the adsorption potential of granular activated carbon can serve as a valuable foundation for further investigations into its effectiveness in adsorbing emerging contaminants.

Keywords: adsorption; emerging contaminants; granular activated carbon; pesticide; pharmaceutical

1. Introduction

In recent years, emerging contaminants have become significant organic pollutants in drinking water, leading to their detection in various public drinking water systems [1]. Natural and anthropogenic trace organic contaminants have also been identified in raw water bodies worldwide. Pesticides and pharmaceutical compounds play crucial roles in enhancing the quality of modern life; unfortunately, these substances also contribute to environmental water contamination [2]. These emerging contaminants are organic compounds that persist in the environment due to their resistance to biodegradation or breakdown processes. Previously, such contaminants, including pharmaceuticals and pesticides, were continuously discharged into the environment without proper recognition owing to limited detection capabilities. However, recent advancements in analytical technology now enable the detection and analysis of trace concentrations in the parts per trillion (ppt) range, leading to the discovery of these issues [3]. Emerging contaminants have the potential to continuously expose ecosystems and public health to bioaccumulation, even at trace concentrations [4]. This ongoing research is vital because the maximum allowable concentration of these contaminants, concerning their long-term exposure to the human body in the environment, remains unknown [4,5].

The treatment of emerging contaminants in raw water presents a significant challenge to researchers due to the diverse chemical characteristics of pesticides and pharmaceutically active compounds. To address this issue, various technologies have been proposed and

evaluated, including biological, physical–chemical treatments, ion exchange, membrane processes, and adsorption, each yielding different results [6–9]. Among these technologies, adsorption using activated carbons is a commonly employed method for removing emerging contaminants. This preference is due to its straightforward design, ease of operation and handling, the possibility of adsorbent regeneration, and the absence of sludge generation [10].

The main objective of this study was to explore the potential of using commercial granular activated carbon for treating and adsorbing nine aqueous emerging contaminants: carbamazepine (CBZ), phenacetin (PHE), pentoxifylline (PEN), norfloxacin (NOR), iprobenfos (IPB), isoprothiolane (ISP), metolachlor (MET), tebuconazole (TEB), and hexaconazole (HEX). We conducted batch experiments to assess the kinetic and isotherm parameters at varying contact times and adsorbent doses. Additionally, we performed batch adsorption experiments and theoretical model investigations to analyze the adsorption kinetics and equilibrium. The results obtained from this adsorption study using granular activated carbon are expected to serve as a valuable foundation for further investigations into the effectiveness of its adsorbent function for removing emerging contaminants.

2. Experimental

2.1. Adsorbents

The adsorbent employed in this study was Norit1240 commercial granular activated carbon (GAC) obtained from Cabot Corporation, Boston, MA, USA. To prepare the GAC, it was dried in an oven (C-Do, Chang Shin Scientific Co., Hwaseongsi, Republic of Korea) at 105 °C for 24 h and then stored in an aluminum bottle. Subsequently, the dried GAC was kept in a desiccator until used for the batch experiments.
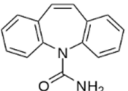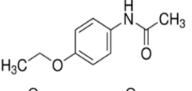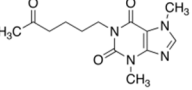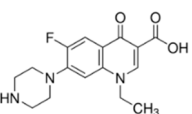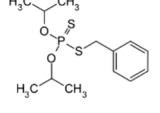
2.2. Chemicals and Reagents

The emerging contaminants utilized in this experiment included CBZ, PHE, PEN, NOR, IPB, ISP, MET, TEB, and HEX, all of which were procured from Sigma-Aldrich, St. Louis, MO, USA. These chemicals were of analytical grade, ensuring the highest available purity. To prepare the stock solutions, 100 mg/L of each contaminant was dissolved in their respective solvents: CBZ in 10% acetonitrile, PHE in 6% acetonitrile, PEN in deionized water, NOR in 0.4% HOAc, IPB in 30% acetonitrile, ISP in 10% acetonitrile, MET in 40% acetonitrile, TEB in 6% acetonitrile, and HEX in 6% acetonitrile solution. The stock solutions were stored in brown bottles to prevent light degradation. For further information on the physical and chemical properties of these emerging contaminants, refer to Table 1.

2.3. Batch Experiments

The removal of emerging contaminants via GAC was assessed through the measurement of both initial and time-dependent concentrations of the contaminants in a batch system. Each trial involved mixing 0.01–2.0 g of GAC with 50 mL of the emerging contaminants solution wi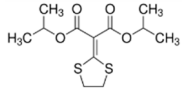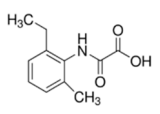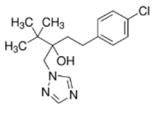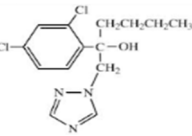thin a 50 mL conical tube. The initial concentration of the contaminants was set at 100 mg/L, and the initial solution pH was adjusted to 7.0 by adding 1.0 N NaOH or H_2SO_4, as required. To promote the reaction, the conical tubes were horizontally agitated on a shaker (Vision Co., Yeosusi, Republic of Korea) at a constant speed of 200 rpm while maintaining the reaction temperature at 25 ± 1 °C. Periodically, 1 mL of the samples was collected and filtered using a 0.2 μm cellulose acetate membrane syringe filter (MACHEREY-NAGEL GmbH & Co. KG, Heilbronn, Germany). Subsequently, the filtered samples were stored in a refrigerator at a temperature below 5 °C until the analysis was conducted. The total volume of withdrawn samples did not exceed 15% of the working volume (50 mL).

Table 1. Physical and chemical properties of the investigated pharmaceutical and pesticide compounds in emerging contaminants.

Compound Type	Compound (CAS-RN)	Classification	Chemical Formula	Chemical Structure	MOL. MASS	log K_{ow}	pK_a
Pharmaceutical compounds	Carbamazepine (298-46-4)	Antiepileptic	$C_{15}H_{12}N_2O$		236.27	2.45	2.3
	Phenacetin (62-44-2)	Pain-relieving, Fever-reducing	$C_{10}H_{13}NO_2$		179.22	1.58	2.1
	Pentoxifylline (6493-05-6)	Circulation problem-reducing	$C_{13}H_{18}N_4O_3$		278.31	0.29	0.97
	Norfloxacin (70458-96-7)	Antibiotic	$C_{16}H_{18}FN_3O_3$		319.33	−1.03	6.22
Pesticide compounds	Iprobenfos (26087-47-8)	Fungicide	$C_{11}H_{17}O_3PS$		260.29	3.21	−8.2
	Isoprothiolane (50512-35-1)	Fungicide, Insecticide	$C_{12}H_{18}O_4S_2$		290.40	2.88	−7
	Metolachlor (87392-12-9)	Herbicide	$C_{15}H_{22}ClNO_2$		283.79	3.13	−1.34
	Tebuconazole (107534-96-3)	Fungicides	$C_{16}H_{22}ClN_3O$		307.82	3.70	2.3
	Hexaconazole (79983-71-4)	Fungicide	$C_{14}H_{17}Cl_2N_3O$		314.21	3.90	2.3

The amount of emerging contaminants per unit mass of adsorbent (q_e) at equilibrium was calculated using the following Equation (1):

$$q_e(\mathrm{mg/g}) = \frac{(C_0 - C_e)V}{W} \tag{1}$$

where C_0 and C_e are initial and equilibrium concentrations of adsorbate (mg/L), respectively; W is the dry mass of adsorbent (g); and V is the volume of solution (L).

2.4. Kinetic Models

To assess the capacity of the adsorption process, pseudo-first-order and pseudo-second-order kinetic models were employed to interpret the experimental data. The pseudo-first-order kinetic model can be expressed using the following Equation (2) [11]:

$$q_t = q_e\left(1 - e^{-k_1 t}\right) \tag{2}$$

where q_e is the amount of adsorbate adsorbed (mg/g) at equilibrium, q_t is the amount of adsorbate adsorbed (mg/g) at time t (h), and k_1 is the pseudo-first-order rate constant (1/h).

The pseudo-second-order kinetic model can be defined as follows in Equations (3) and (4) [11]:

$$\frac{t}{q_t} = \frac{1}{k_2 \cdot q_e{}^2} + \frac{t}{q_e} \tag{3}$$

And

$$\frac{q_t}{t} = \frac{h}{1 + k_2 q_e t} \tag{4}$$

where h (g/mg·h) is the initial sorption rate, and k_2 (g/mg·h) is the rate constant for the pseudo-second-order equation.

In the adsorption process, the kinetic data were analyzed using the Weber and Morris intraparticle diffusion models to elucidate the diffusion mechanism. The dynamic process of solid–liquid adsorption can be described in three steps. The Weber and Morris intraparticle diffusion model can be expressed as follows in Equation (5) [12]:

$$q_t = k_p t^{1/2} + C \tag{5}$$

where k_p is the intra-particle diffusion rate constant (mg/g·h$^{1/2}$), and C is a constant relating to the thickness of the boundary layer (mg/g), which can be determined from the plot of q_t versus $t^{1/2}$. In general, adsorption in this model involves the following steps: (1) migration of adsorbate from the bulk of the solution to the surface of the adsorbent (bulk diffusion), (2) the diffusion of the adsorbate through the boundary layer to the surface of the adsorbent (film diffusion), (3) the transport of the adsorbate from the surface to the interior pores of the adsorbent (intra-particle diffusion), and (4) adsorption at an active site on the surface of adsorbent (chemical reaction via ion-exchange complexation).

2.5. Equilibrium Isotherm Model

The equilibrium adsorption isotherm holds fundamental significance in optimizing the use of adsorbents. Analyzing isotherm data by fitting the data to models is a crucial step in identifying a suitable model for the design of adsorption systems. In this study, Langmuir and Freundlich isotherm models were employed to determine the adsorption equilibrium for various emerging contaminants.

The Langmuir model equation is based on the assumptions that the adsorption site is homogeneous and that each site accommodates one adsorbate molecule or ion; adsorption is monolayer coverage, and there is no interaction between adsorbed molecules or ions [13]. The Freundlich model equation is an empirical equation used for heterogeneous systems and is not restricted to formation of a monolayer [13]. The Langmuir isotherm equations can be expressed as follows in Equation (6):

$$q_e = \frac{q_m b_L C_e}{1 + b_L C_e} \tag{6}$$

and the Freundlich isotherm equations can be expressed as follows in Equation (7):

$$q_e = K_F C_e{}^{1/n} \tag{7}$$

where C_e is the equilibrium concentration of emerging contaminants (mg/L), q_e is the number of emerging contaminants adsorbed at equilibrium (mg/g), q_m is the maximum adsorption capacity (mg/g), and b_L (L/g) is the Langmuir isotherm constant. K_F (mg/g) (L/mg)$^{1/n}$ and $1/n$ (dimensionless) are Freundlich constants representing adsorption capacity and adsorption intensity (level of favorability), respectively. When $1/n < 0.01$ between adsorbate and adsorbent, adsorption is pseudo-irreversible; $0.01 < 1/n < 0.1$, strongly favorable; $0.1 < 1/n < 0.5$, favorable; $0.5 < 1/n < 1$, pseudo-linear; $1/n = 1$, linear; and $1/n > 1$, unfavorable [14].

2.6. Analysis

The Brunauer, Emmett, and Teller (BET) surface area and pore size distributions were measured using a Surface Area Analyzer ASAP 2010 (Micromeritics, Norcross, GA, USA) through nitrogen adsorption at -196 °C in the range of relative pressure (P/P$_0$). The pore volume distribution as a function of pore size was calculated based on the Barret, Joyner, and Halenda (BJH) method.

Methylene blue capacity analysis was performed in Erlenmeyer flasks (100 mL) using 25 mL solutions of dye with an initial concentration of 500 mg/L. A mass of 0.1 g of GAC adsorbent was added to the solution and placed in a shaker at 200 rpm with a constant reaction temperature of 25 ± 1 °C for 30 min. The concentration of methylene blue in the supernatant solution before and after adsorption was determined using a UV-VIS spectrophotometer (Vision Co., Yeosusi, Republic of Korea) at 665 nm.

Iodine number analysis was performed in Erlenmeyer flasks (100 mL) with solutions of iodine (50 mL) at initial concentrations of 0.1 N. A mass of 0.5 g of adsorbent GAC was added to the solution and placed in a shaker at 200 rpm with a constant reaction temperature of 25 ± 1 °C for 15 min. The iodine in the supernatant solution after adsorption was added to 1.0 mL soluble starch (1%), and the concentration of iodine was determined using 0.1 M sodium thiosulfate by the titration method.

The solid addition method was used to determine the zero surface charge characteristics (pH$_{pzc}$) of the GAC [15]. The initial pH (pH$_i$) of each solution was adjusted to between 2.0 and 12.0 by adding 0.1 N HCl and 0.1 N NaOH solutions using deionized water. The volume of the solution in each capped glass vial was adjusted to 50 mL. The pH$_i$ of each solution was accurately recorded, and 0.5 g of unique GAC was added to each vial. The tubes were horizontally agitated on a shaker at 200 rpm with a constant reaction temperature of 25 ± 1 °C for 24 h. The final pH (pH$_f$) of the supernatant liquid was noted. The ΔpH, the difference between the pH$_i$ and pH$_f$, was plotted against pH$_i$. The point of intersection of the resulting curve with the abscissa, at which ΔpH = 0, determined pH$_{pzc}$.

The concentrations of emerging contaminants were determined in the collected samples using Ultra Performance Liquid Chromatography UPLC-Orbitrap MS (EQuan Max, Thermo Fisher Scientific Inc., Waltham, MA, USA) with a Thermo Scientific™ Hypersil GOLD aQ™ pre-concentration column (20×2.1 mm, 12 μm particle size) and a Thermo Scientific™ Hypersil GOLD™ analytical column (50×2.1 mm, 1.9 μm particle size). The allowable liquid sample injection range was 1.0 to 20 mL, and the sample injection amount was set at 1.0 mL after considering the WHO guidelines, equipment sensitivity, peak shape, and concentration ratio of online injection. The standard material for the calibration curve and all the samples used in the analysis were filtered through a 0.2 μm GHP (hydrophilic polypropylene) membrane syringe filter.

3. Results and Discussion

3.1. Characterization of the Adsorbent

The activated carbon Norit1240 was derived from bituminous coal, known for its high surface area and significant adsorption capacity. Its porous properties, including BET surface area, pore size, pore volume, iodine number, and methylene blue number, are presented in Table 2. The BET surface area and micro-pore areas were determined to be 930.5 m^2/g and 676.0 m^2/g, respectively. The average pore widths from the BJH adsorption and desorption measurements were also recorded. Figure 1 illustrates the distributions of pore volume (a), pore area (b), and N$_2$ adsorption–desorption isotherms (c). The isotherm exhibits the characteristics of a typical type I isotherm, indicating the presence of microporous material in Norit1240. Notably, the slope changes in the region around 0.1 and 0.9, suggesting unique adsorption characteristics in this specific range.

Table 2. Physicochemical characterization of sorbent for commercial Norit1240 GAC.

| Characteristics	Norit 1240
Source material	Bituminous coal
BET Surface area (m^2/g)	930.4871
Micro-pore Surface area (m^2/g)	676.0105
Total pore volume (cm^3/g)	0.5710
Micro-pore volume (cm^3/g)	0.3113
Adsorption average pore width (nm)	2.4546
BJH Adsorption average pore diameter (nm)	3.9258
BJH Desorption average pore diameter (nm)	4.1566
Granulation (mm)	0.4–1.7
Methylene blue (mL/g)	153.44 ± 0.76
Iodine number (mg/g)	680.63 ± 12.10
Hardness (%)	>95%
pH_{pzc}	10.0
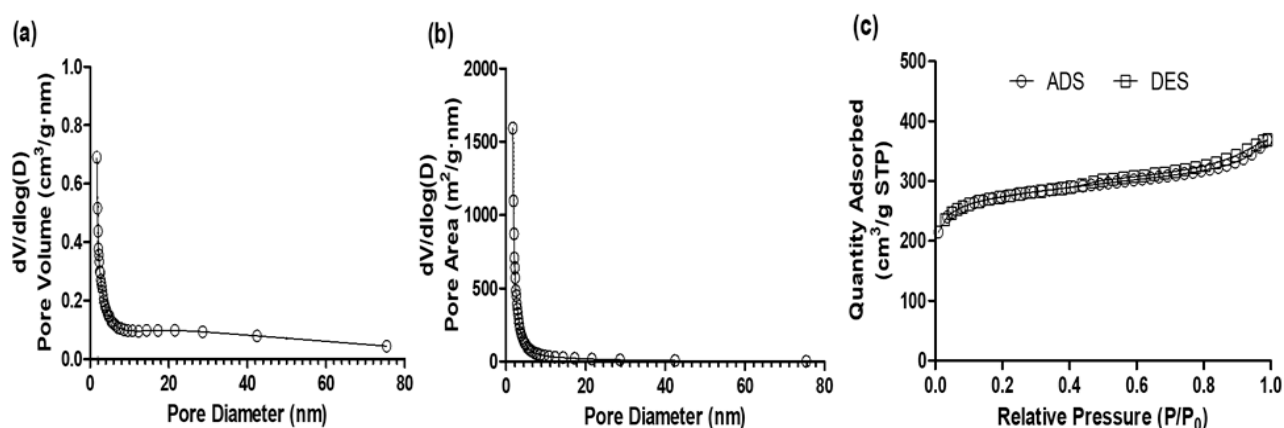
Figure 1. Distributions of (**a**) pore-volume and (**b**) pore-area with pore-size diameter, and (**c**) nitrogen adsorption–desorption isotherm at −196 °C for granular activated carbon.

3.2. Adsorption Kinetic Model

The kinetics parameters of emerging contaminants' adsorption are presented in Table 3 using the pseudo-first-order and pseudo-second-order kinetic models. In all cases, the concentrations of the nine emerging contaminants in the solution decreased rapidly within the first 12 h and continued to decrease gradually until reaching equilibrium within 24 h. Table 3 provides the calculated parameters of the kinetic models for each adsorbate, along with the corresponding correlation coefficients (r^2) for the data and the two kinetic models, offering a comprehensive summary of the adsorption of emerging contaminants.

Based on the correlation coefficients, it appears that the adsorptions of all emerging contaminants onto the GAC are better represented by pseudo-second-order kinetics. Although reasonable correlations were observed for the pseudo-first-order rate model, the pseudo-second-order model provides a more suitable fit to the experimental data. Consequently, it is assumed that physical–chemical adsorption is involved in the adsorption process. Figure 2 illustrates the kinetics of emerging contaminants' adsorption, presenting the equilibrium concentration (C_e) for each adsorbate over time (*h*). The graph visually portrays the adsorption behavior of the contaminants, further supporting the findings obtained from the kinetic model analyses. The initial sorption rates for the emerging contaminants exhibited the fastest adsorption rates and were ranked in descending order as follows: TEB (121.27 g/mg·h) > NOR (99.61 g/mg·h) > IPR (89.95 g/mg·h) > CBZ (78.39 g/mg·h) > ISO (68.44 g/mg·h) > PHE (63.19 g/mg·h) > HEX (62.33 g/mg·h) > PEN (55.27 g/mg·h) > MET (47.70 g/mg·h). However, when considering the adsorption capacity, differences were observed for the initial sorption rates. Notably, some adsorbates, such as NOR, IPR, MET,

and HEX, did not undergo complete adsorption. This variation in adsorption capacity indicates different adsorption mechanisms between the adsorbates and the adsorbent, signifying complexities in their interactions during the adsorption process.

Table 3. Kinetic parameters of various emerging contaminants for pseudo-first- order model and pseudo-second-order model.

	Initial Concentration (mg/L)	$q_{e,exp}$ (mg/g)	Pseudo First Order Kinetic Model			Pseudo Second Order Kinetic Model			
			$q_{e,cal}$ (mg/g)	k_1 (h)	r^2	$q_{e,cal}$ (mg/g)	$k_2 \times 10^3$ (g/mg·h)	Initial Sorption Rate (g/mg·h)	r^2
Carbamazepine	100	97.66	89.45	0.3104	0.9935	106.11	6.962	78.39	0.9934
Phenacetin	100	97.91	90.03	0.403	0.9850	106.52	5.568	63.19	0.9912
Pentoxifylline	100	97.75	82.92	0.1725	0.9735	103.13	5.197	55.27	0.9981
Norfloxacin	100	77.32	48.66	0.2463	0.8440	79.59	15.726	99.61	0.9987
Iprobenfos	100	80.03	59.45	0.2343	0.9526	82.39	13.252	89.95	0.9992
Isoprothiolane	100	99.29	106.23	0.4193	0.9847	106.77	6.003	68.44	0.9974
Metolachlor	100	69.77	56.69	0.1709	0.9740	72.36	9.108	47.70	0.9947
Tebuconazole	100	99.07	91.05	0.3903	0.9931	102.67	11.504	121.27	0.9982
Hexaconazole	100	75.37	49.83	0.1636	0.8609	77.75	10.312	62.33	0.9957
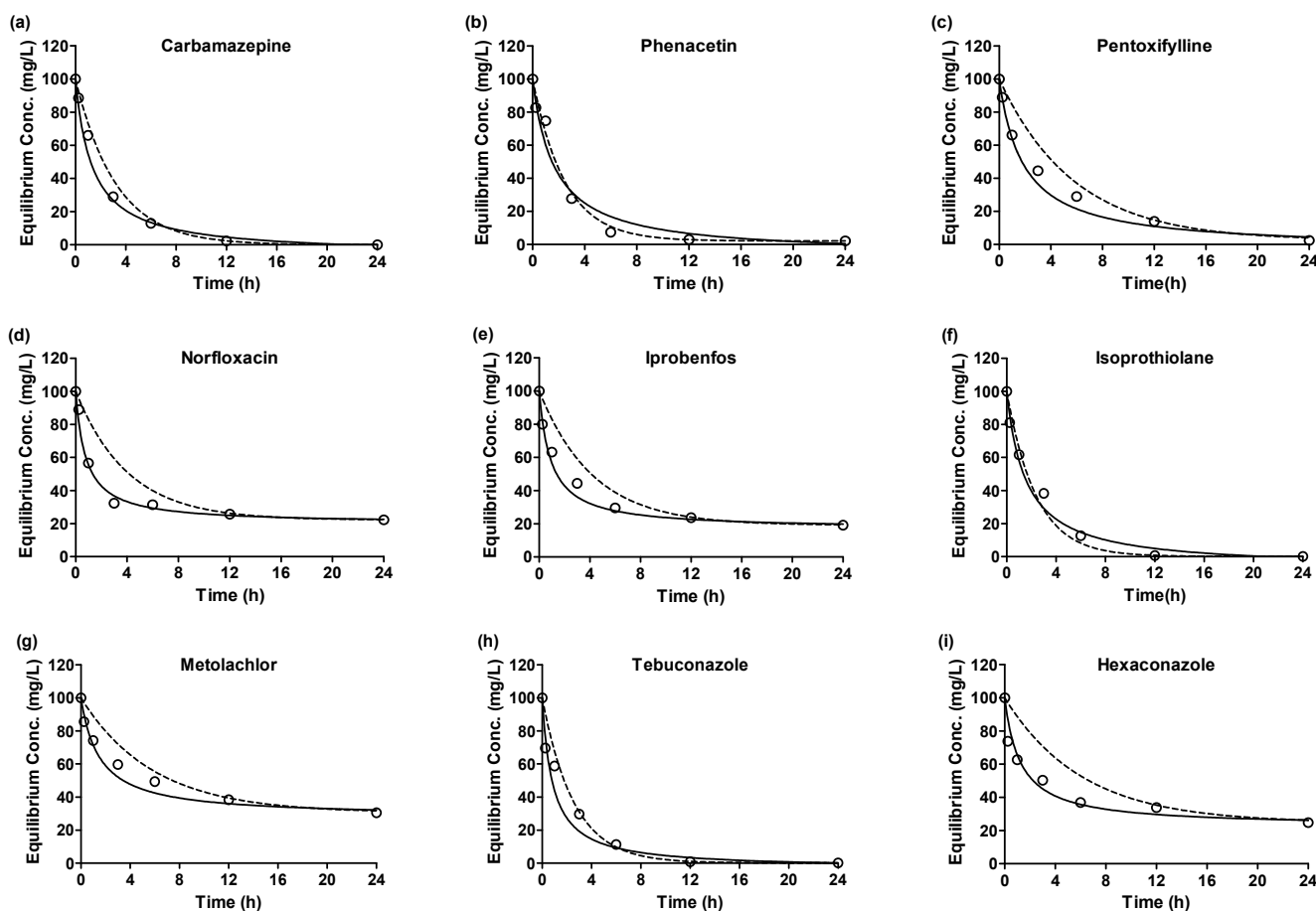
Figure 2. Adsorption kinetics plots emerging contaminants (**a**) carbamazepine, (**b**) phenacetin, (**c**) pentoxifylline, (**d**) norfloxacin, (**e**) iprobenfos, (**f**) isoprothiolane, (**g**) metolachlor, (**h**) tebuconazole, (**i**) hexaconazole by granular active carbon of experiments data, pseudo-1st-order model and pseudo-2nd-order model (empty circle: experiment data, dot-line: pseudo-1st-order, solid-line: pseudo-2nd-order).

3.3. Diffusion Mechanism

Among the kinetic models, the Weber and Morris intraparticle diffusion model is recognized as the most suitable for describing adsorption via physical sorption. The plots of q_t vs. $t^{1/2}$ are presented for the adsorption of emerging contaminants onto adsorbents at a 100 mg/L concentration (Figure 3) and model parameter values are shown in Table 4.
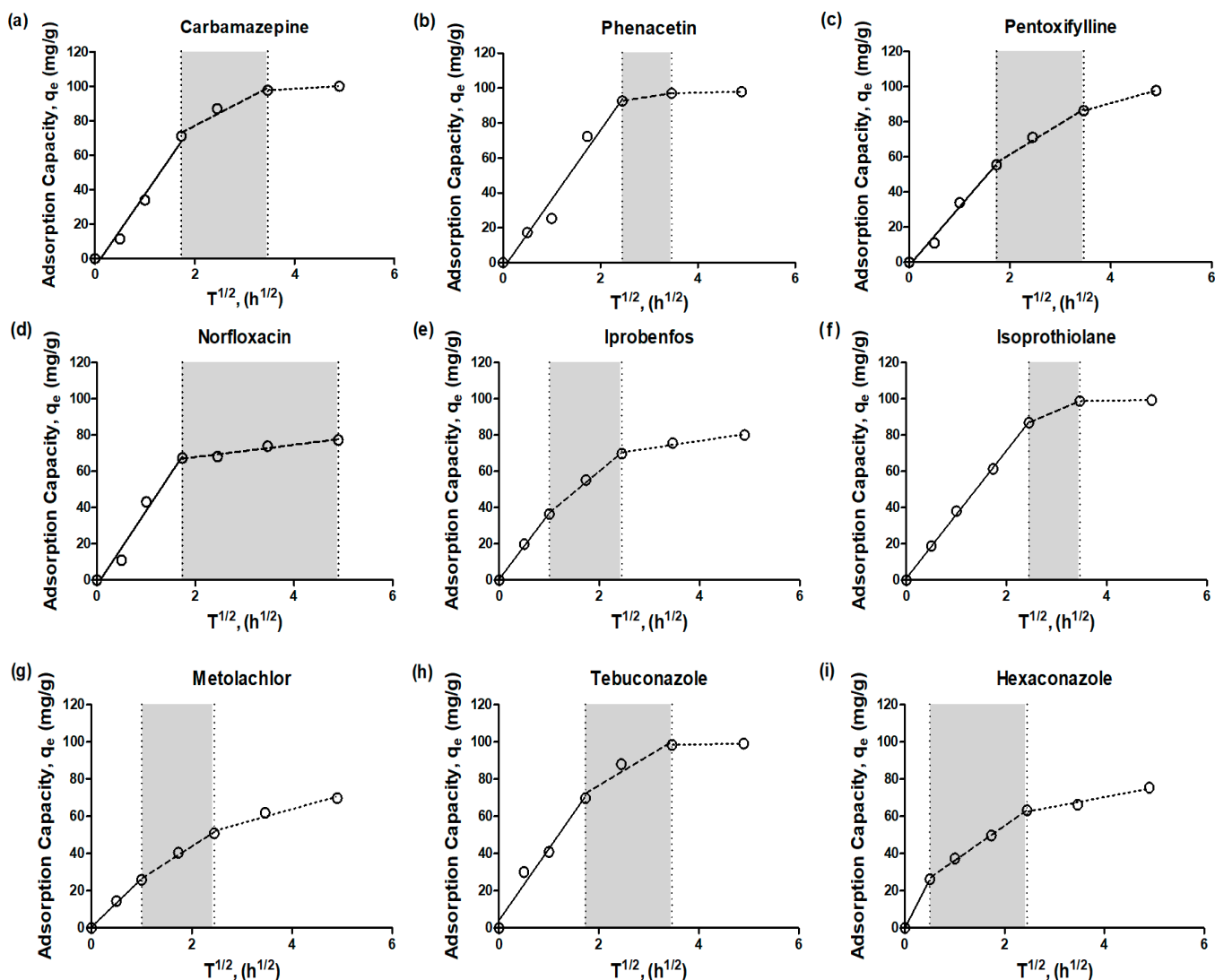

Figure 3. Intra-particle diffusion model (Weber and Morris model) for emerging contaminants (**a**) carbamazepine, (**b**) phenacetin, (**c**) pentoxifylline, (**d**) norfloxacin, (**e**) iprobenfos, (**f**) isoprothiolane, (**g**) metolachlor, (**h**) tebuconazole, (**i**) hexaconazole) adsorption by granular active carbon (empty circle: experiment data, solid-line: 1st-stage, dash-line: 2nd-stage, dot-line: 3rd-stage).

The intraparticle plots exhibited an asymptotic pattern, which could be divided into a multi-linearity pattern comprising three distinct stages in the adsorption process of GAC. This model proves effective when the external solute concentration lies within the plateau region of the adsorption isotherm of the material. The plots displayed consistent features across all cases, with three linear segments followed by a plateau. The first segment, represented by a solid line with a short adsorption period, indicated the involvement of outer diffusion during the early stage of adsorption for the emerging contaminants. The second segment, represented by a dashed line, corresponded to inner diffusion, signifying the transport of adsorbate from the external surface to the interior pores of the adsorbent. The third segment, illustrated by a dotted line, characterized the final plateau, which

indicated a state of adsorption equilibrium, where the adsorption rate and desorption rate reached a balance [16].

Table 4. Coefficients of various emerging contaminants for Weber–Morris diffusion model.

	First Stage (Outer Diffusion)		Second Stage (Inner Diffusion)		Third Stage (Adsorption Equilibrium)	
	$K_{i,1}$ (mg/g·h$^{1/2}$)	r^2	$K_{i,2}$ (mg/g·h$^{1/2}$)	r^2	$K_{i,3}$ (mg/g·h$^{1/2}$)	r^2
Carbamazepine	41.91	0.9779	15.02	0.9552	1.631	1.0000
Phenacetin	39.61	0.9700	4.317	1.0000	0.6133	1.0000
Pentoxifylline	33.22	0.9870	17.54	0.9882	8.022	1.0000
Norfloxacin	40.96	0.9722	3.394	0.9577	-	-
Iprobenfos	36.41	0.9973	22.99	0.9958	4.136	0.9688
Isoprothiolane	35.17	0.9989	11.72	1.0000	0.3833	1.0000
Metolachlor	25.94	0.9956	17.21	0.9924	7.565	0.9632
Tebuconazole	38.50	0.9734	16.06	0.9357	0.5157	1.0000
Hexaconazole	52.42	1.0000	18.66	0.9976	5.064	0.9679

In the section marked with a gray background (dashed line), it was observed that the time required for inner diffusion varied depending on the type of adsorbent and adsorbate. Particularly, NOR exhibited different periods of inner and outer diffusion compared to other emerging contaminants. As we mentioned earlier, this discrepancy could be attributed to different intra-diffusion phases for each emerging contaminant, leading to enhanced resistance in terms of diffusion between the adsorbent and adsorbate. For all adsorbates, the adsorption plots of emerging contaminants did not intersect at the origin, indicating that intraparticle diffusion alone was not the sole rate-limiting step. Instead, external mass transfer also played a significant role in influencing the adsorption process [17,18]. Indeed, Figure 3 clearly demonstrates that the time required for inner diffusion is significantly longer than that for outer diffusion. This observation suggests that the adsorption process is influenced by both outer and inner diffusion, indicating a control mechanism involving both types of diffusion. As a result, the overall mass transfer in the adsorption process appears to be predominantly governed by inner diffusion rather than outer diffusion.

This finding emphasizes the crucial role of intra-particle diffusion in the adsorption of emerging contaminants onto the adsorbents studied in this research. The extended time required for inner diffusion indicates that the transport of adsorbate from the external surface to the interior pores of the adsorbent plays a key role in determining the overall rate of adsorption. Understanding and characterizing the contribution of both inner and outer diffusion are essential for optimizing and designing effective adsorption systems for the removal of emerging contaminants.

3.4. Equilibrium of Emerging Contaminants

The equilibrium adsorption isotherm plays a fundamental role in optimizing the use of adsorbents, and analyzing isotherm data by fitting it to various isotherm models is a crucial step in identifying the most suitable model for the design of the adsorption system. The distribution of emerging contaminants between the adsorbent and solution at equilibrium was expressed using isotherm equations (Figure 4). Two widely used forms in adsorption equilibrium conditions are the Freundlich and Langmuir isotherm models. The calculated values of the isotherm parameters (q_m, b_L, K_F, and n), along with the coefficient of determination r^2 values, are summarized in Table 5. In all cases, the Freundlich isotherm consistently displayed a higher correlation coefficient than the Langmuir isotherm, implying that the Freundlich isotherm provides a more suitable description of the data for the adsorption of emerging contaminants. This higher correlation coefficient indicates a better fit of the experimental data to the Freundlich isotherm model. The Langmuir isotherm model is typically associated with monolayer sorption on homogeneous surface

sites, where all pore sites possess equal affinity for the adsorbate [19]. On the other hand, the Freundlich isotherm is more suitable for describing the adsorption of organic compounds on heterogeneous surface sorbents, such as activated carbon, and is generally recognized for multi-layer sorption [20].
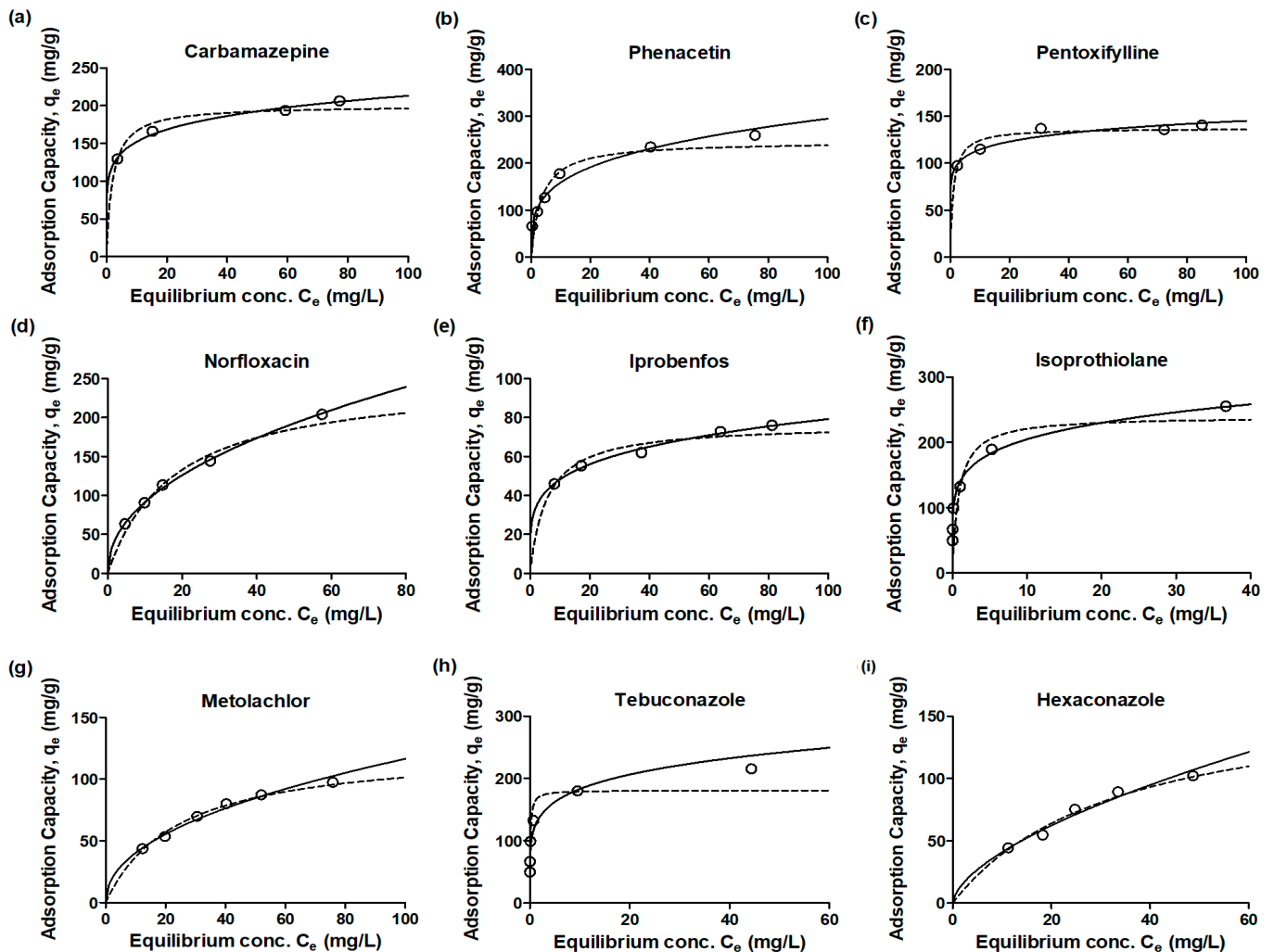

Figure 4. Adsorption isotherm plots for emerging contaminants (**a**): carbamazepine, (**b**): phenacetin, (**c**): pentoxifylline, (**d**): norfloxacin, (**e**): iprobenfos, (**f**): isoprothiolane, (**g**): metolachlor, (**h**): tebuconazole, (**i**): hexaconazole) by granular active carbon experiment data, Langmuir and Freundlich models (empty circle: experiment data, dot-line: Langmuir model; solid-line: Freundlich model).

The slope range observed for the equilibrium concentration versus adsorption capacity was between 0 and 1, indicating an increase in surface heterogeneity as the slope approached zero. Moreover, the values close to zero for the adsorption intensity parameter ($1/n$) suggested a strong chemisorption process [14,20]. The low $1/n$ values (<0.2) obtained for CBZ, PEN, ISO, and TEB indicated chemisorption as the dominant adsorption mechanism for these contaminants. Conversely, the high $1/n$ values (>0.4) observed for NOR, MET, and HEX suggested physisorption as the predominant adsorption mechanism for these contaminants. The results of this study highlight the importance of considering adsorption properties to determine the most suitable adsorbent for the specific adsorption mechanism involved in removing emerging contaminants using activated carbon. Understanding the adsorption mechanisms can aid in selecting the appropriate adsorbent and optimizing the efficiency of the adsorption process for different types of emerging contaminants.

Table 5. Isotherm parameters of various emerging contaminants for Langmuir and Freundlich models.

		Langmuir Model			Freundlich Model		
	$q_{e,exp}$ (mg/g)	$q_{e,cal}$ (mg/g)	b_L (L/mg)	r^2	K_F (mg/g) (L/mg)$^{1/n}$	n	r^2
Carbamazepine	206.34	200.08	0.495	0.9574	108.671	6.839	0.9901
Phenacetin	248.89	245.87	0.293	0.9658	86.011	3.739	0.9827
Pentoxifylline	140.83	137.27	0.957	0.9187	90.447	9.734	0.9411
Norfloxacin	204.16	251.51	0.056	0.9878	31.538	2.162	0.9980
Iprobenfos	76.05	76.45	0.177	0.9443	29.365	4.640	0.9905
Isoprothiolane	255.36	239.70	1.162	0.9537	139.324	5.976	0.9905
Metolachlor	97.44	125.59	0.042	0.9867	13.949	2.170	0.9848
Tebuconazole	215.52	181.02	8.725	0.8769	123.187	5.809	0.9623
Hexaconazole	158.56	170.79	0.030	0.9658	10.088	1.647	0.9715

3.5. Relationship of between Emerging Contaminants and Adsorption

The adsorption of emerging contaminants onto adsorbents is significantly influenced by factors such as hydrophobicity, hydrophilicity, molecular weight, and acid dissociation constant (pK_a) of the compound (Table 6). A general rule of thumb, as explained by Rogers [21], suggests that the octanol-water partition coefficient (K_{OW}) can be used to estimate adsorption potential. Specifically, log K_{OW} values below 2.5 indicate low adsorption potential, values between 2.5 and 4 indicate medium adsorption potential, and values above 4 indicate high adsorption potential. Additionally, the pK_a, determined by the functional group of a compound, plays a crucial role in the chemisorption and/or electrostatic adsorption of emerging contaminants. For instance, at a pH higher than the pK_a, the phenolic hydroxyl group of compounds becomes negatively charged, leading to charge repulsion with negatively charged adsorbents [22]. This charge repulsion can also occur between negatively charged emerging contaminants and negatively charged adsorbents, hindering the removal of emerging contaminants. Considering the hydrophobicity, pK_a, and other molecular properties of emerging contaminants is essential when selecting the appropriate adsorbent and designing effective adsorption processes for the removal of these contaminants from water systems.

Table 6. Relationship parameters for emerging contaminants in adsorption.

Compound	Octanol-Water Partition Coefficient (log K_{ow})	Acid Dissociation Constant (pK_a)	Maximum Adsorption Capacity (q_{max}; mg/g)	Pseudo-2nd-Order Rate Constant (k_2; g/mg·h)
Carbamazepine	2.45	2.3	206.34	0.0070
Phenacetin	1.58	2.1	248.89	0.0056
Pentoxifylline	0.29	0.97	140.83	0.0052
Norfloxacin	−1.03	6.22	204.16	0.0157
Iprobenfos	3.21	−8.2	76.05	0.0133
Isoprothiolane	2.88	−7	255.36	0.0060
Metolachlor	3.13	−1.34	97.44	0.0091
Tebuconazole	3.7	2.3	215.52	0.0115
Hexaconazole	3.9	2.3	158.56	0.0103

The properties of emerging contaminants can significantly influence their behaviors during the adsorption process. Previous research has demonstrated that adsorption can effectively remove emerging contaminants [23–26]. However, only a limited number of studies have explored the relationship between adsorption and the properties of emerging contaminants [27]. Figure 5 illustrates the relationship between the pseudo-second-order rate constant (k_2, g/mg·h) of emerging contaminants during adsorption and their properties in terms of log K_{ow}. The results show a relatively linear correlation between the rate constant and log K_{ow} ($r^2 = 0.5710$). Previous studies have attempted to directly relate log

K_{ow} to observed adsorption rates and found such relations in systems containing hydrophobic solutes and a hydrophobic adsorbent [27]. Since the GAC surface properties generally appear hydrophobic, increasing log K_{ow} values were associated with higher adsorption rates on GAC. Figure 6 depicts the relationship between the maximum adsorption capacity (q_{max}, mg/g) of emerging contaminants during adsorption and their properties in terms of pK_a. The results show a relatively linear correlation between the removal of emerging contaminants during adsorption and pK_a ($r^2 = 0.6055$). High pK_a values indicate strong acidity and correspond to high pH_{pzc} values on the GAC surface. Consequently, adsorption capacity increased for contaminants with high pK_a values. Emerging contaminants with both high pK_a and log K_{ow} values could be easily removed through adsorption, primarily due to electrostatic attraction with the positively charged adsorbent. These findings highlight the importance of considering the properties of emerging contaminants, such as log K_{ow} and pK_a, in predicting their adsorption behavior and designing effective adsorption processes for their removal from water systems. Understanding these relationships can aid in the selection of appropriate adsorbents and the optimization of adsorption systems for the removal of specific emerging contaminants.
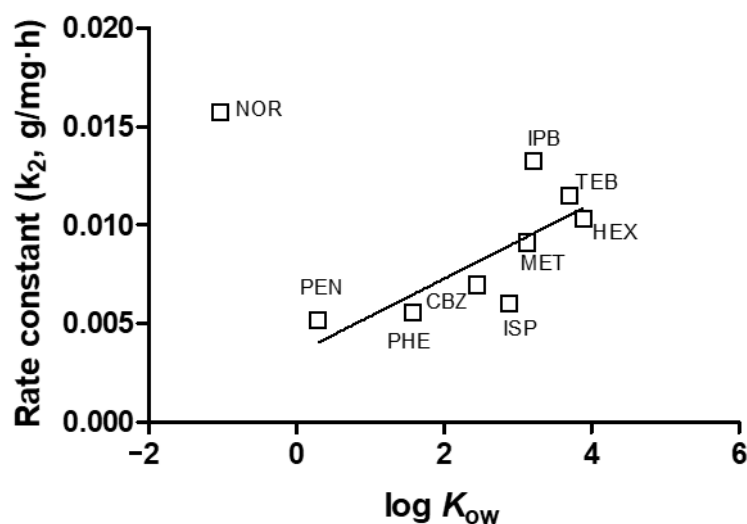

Figure 5. Relationship between emerging contaminants pseudo 2nd order rate constant during adsorption and log K_{ow}.
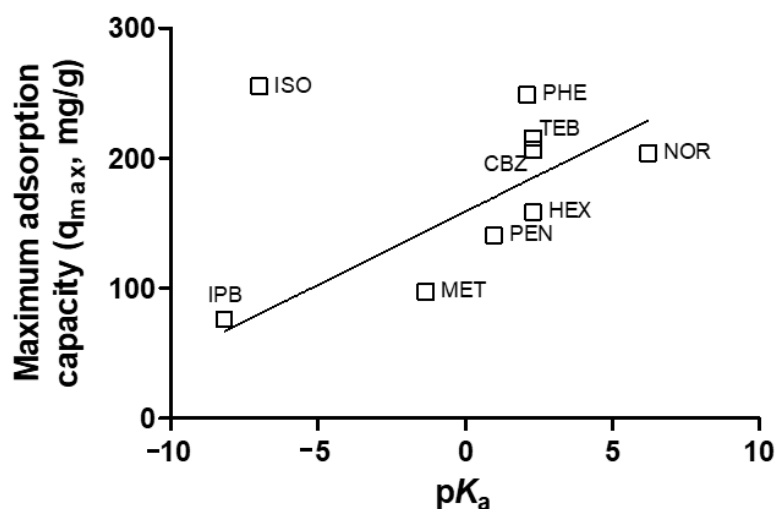

Figure 6. Relationship between emerging contaminants maximum adsorption capacity during adsorption and pK_a.

4. Conclusions

In this study, the adsorption potential of granular activated carbon (GAC) for nine emerging contaminants was investigated. The findings revealed that GAC achieved adsorption equilibrium within 12 h, with maximum adsorption capacities ranging from 76 to 206 mg/g. The adsorption processes were better described by the pseudo-second-order kinetic equation, and they were governed by outer diffusion at the initial stage, followed by inner diffusion during subsequent periods. The adsorption isotherms demonstrated that the adsorption of emerging contaminants adhered more closely to the Freundlich model than the Langmuir model. Furthermore, the molecular properties of the emerging contaminants, such as K_{ow} and pK_a, were correlated with their behaviors during adsorption, influencing the rate constant and maximum adsorption capacity of the removal process. Overall, the results from this adsorption study of granular activated carbon provide valuable insights for further exploring the effectiveness of the adsorbent in removing emerging contaminants.

Author Contributions: Conceptualization, D.P.; Methodology, S.-H.L. and N.K.; Invesigation, S.-H.L.; Data curation, S.-H.L. and N.K.; Writing-original drafe, S.-H.L. and N.K.; Review & editing, D.P. All authors have read and agreed to the published version of the manuscript.

Data Availability Statement: All data generated or analyzed during this study are included in this published article.

Conflicts of Interest: The authors declare no conflict of interest.

References

1. Yu, Z.; Peldszus, S.; Huck, P.M. Adsorption characteristics of selected pharmaceuticals and an endocrine disrupting compound—Naproxen, carbamazepine and nonylphenol—On activated carbon. *Water Res.* **2008**, *42*, 2873–2882. [CrossRef] [PubMed]
2. Farré, M.L.; Pérez, S.; Kantiani, L.; Barceló, D. Fate and toxicity of emerging pollutants, their metabolites and transformation products in the aquatic environment. *TrAC Trends Anal. Chem.* **2008**, *27*, 991–1007. [CrossRef]
3. Daughton, C.G. Non-regulated water contaminants: Emerging research. *Environ. Impact Assess. Rev.* **2004**, *24*, 711–732. [CrossRef]
4. Schriks, M.; Heringa, M.B.; van der Kooi, M.M.E.; de Voogt, P.; van Wezel, A.P. Toxicological relevance of emerging contaminants for drinking water quality. *Water Res.* **2010**, *44*, 461–476. [CrossRef] [PubMed]
5. Bolong, N.; Ismail, A.F.; Salim, M.R.; Matsuura, T. A review of the effects of emerging contaminants in wastewater and options for their removal. *Desal.* **2009**, *239*, 229–246. [CrossRef]
6. Comerton, A.M.; Andrews, R.C.; Bagley, D.M.; Yang, P. Membrane adsorption of endocrine disrupting compounds and pharmaceutically active compounds. *J. Membr. Sci.* **2007**, *303*, 267–277. [CrossRef]
7. Rakić, V.; Rac, V.; Krmar, M.; Otman, O.; Auroux, A. The adsorption of pharmaceutically active compounds from aqueous solutions onto activated carbons. *J. Hazard. Mater.* **2015**, *282*, 141–149. [CrossRef]
8. Rivera-Utrilla, J.; Sánchez-Polo, M.; Ferro-García, M.Á.; Prados-Joya, G.; Ocampo-Pérez, R. Pharmaceuticals as emerging contaminants and their removal from water. A review. *Chemosphere* **2013**, *93*, 1268–1287. [CrossRef]
9. Rosal, R.; Rodríguez, A.; Perdigón-Melón, J.A.; Petre, A.; García-Calvo, E.; Gómez, M.J.; Agüera, A.; Fernández-Alba, A.R. Occurrence of emerging pollutants in urban wastewater and their removal through biological treatment followed by ozonation. *Water Res.* **2010**, *44*, 578–588. [CrossRef]
10. Rodriquez-Narvaez, O.M.; Peralta-Hernandez, J.M.; Goonetilleke, A.; Bandala, E.R. Treatment technologies for emerging contaminants in water: A review. *Chem. Eng. J.* **2017**, *323*, 361–380. [CrossRef]
11. Ho, Y.S.; McKay, G. Sorption of dye from aqueous solution by peat. *Chem. Eng. J.* **1998**, *70*, 115–124. [CrossRef]
12. Weber, W.J.; Morris, J.C. Kinetics of adsorption on carbon from solution. *J. Sanit. Eng. Div.* **1963**, *89*, 31–60. [CrossRef]
13. Tan, I.A.W.; Hameed, B.H.; Ahmad, A.L. Equilibrium and kinetic studies on basic dye adsorption by oil palm fibre activated carbon. *Chem. Eng. J.* **2007**, *127*, 111–119. [CrossRef]
14. Tseng, R.-L.; Wu, F.-C. Inferring the favorable adsorption level and the concurrent multi-stage process with the freundlich constant. *J. Hazard. Mater.* **2008**, *155*, 277–287. [CrossRef]
15. Khan, M.A.; Lee, S.-H.; Kang, S.; Paeng, K.-J.; Lee, G.; Oh, S.-E.; Jeon, B.-H. Adsorption studies for the removal of methyl tert-butyl ether on various commercially available gacs from an aqueous medium. *Sep. Sci. Technol.* **2011**, *46*, 1121–1130. [CrossRef]
16. Lu, S.; Song, Z.; He, J. Diffusion-controlled protein adsorption in mesoporous silica. *J. Phys. Chem. B* **2011**, *115*, 7744–7750. [CrossRef]

17. Gao, Q.; Zhu, H.; Luo, W.-J.; Wang, S.; Zhou, C.-G. Preparation, characterization, and adsorption evaluation of chitosan-functionalized mesoporous composites. *Microporous Mesoporous Mater.* **2014**, *193*, 15–26. [CrossRef]

18. Vinhal, J.O.; Lage, M.R.; Carneiro, J.W.M.; Lima, C.F.; Cassella, R.J. Modeling, kinetic, and equilibrium characterization of paraquat adsorption onto polyurethane foam using the ion-pairing technique. *J. Environ. Manag.* **2015**, *156*, 200–208. [CrossRef]

19. Saeed, M.M.; Rusheed, A.; Ahmed, N. Modeling of iron adsorption on htta-loaded polyurethane foam using freundlich, langmuir and d-r isotherm expressions. *J. Radioanal. Nucl. Chem.* **1996**, *211*, 283–292. [CrossRef]

20. Foo, K.Y.; Hameed, B.H. Insights into the modeling of adsorption isotherm systems. *Chem. Eng. J.* **2010**, *156*, 2–10. [CrossRef]

21. Rogers, H.R. Sources, behaviour and fate of organic contaminants during sewage treatment and in sewage sludges. *Sci. Total Environ.* **1996**, *185*, 3–26. [CrossRef] [PubMed]

22. Schäfer, A.I.; Akanyeti, I.; Semião, A.J.C. Micropollutant sorption to membrane polymers: A review of mechanisms for estrogens. *Adv. Colloid Interface Sci.* **2011**, *164*, 100–117. [CrossRef]

23. Boyd, G.R.; Reemtsma, H.; Grimm, D.A.; Mitra, S. Pharmaceuticals and personal care products (ppcps) in surface and treated waters of Louisiana, USA and Ontario, Canada. *Sci. Total Environ.* **2003**, *311*, 135–149. [CrossRef] [PubMed]

24. Loraine, G.A.; Pettigrove, M.E. Seasonal variations in concentrations of pharmaceuticals and personal care products in drinking water and reclaimed wastewater in southern california. *Environ. Sci. Technol.* **2006**, *40*, 687–695. [CrossRef] [PubMed]

25. Ternes, T.A.; Meisenheimer, M.; McDowell, D.; Sacher, F.; Brauch, H.-J.; Haist-Gulde, B.; Preuss, G.; Wilme, U.; Zulei-Seibert, N. Removal of pharmaceuticals during drinking water treatment. *Environ. Sci. Technol.* **2002**, *36*, 3855–3863. [CrossRef]

26. Vieno, N.M.; Härkki, H.; Tuhkanen, T.; Kronberg, L. Occurrence of pharmaceuticals in river water and their elimination in a pilot-scale drinking water treatment plant. *Environ. Sci. Technol.* **2007**, *41*, 5077–5084. [CrossRef]

27. Westerhoff, P.; Yoon, Y.; Snyder, S.; Wert, E. Fate of endocrine-disruptor, pharmaceutical, and personal care product chemicals during simulated drinking water treatment processes. *Environ. Sci. Technol.* **2005**, *39*, 6649–6663. [CrossRef]